This document was prepared in conjunction with work accomplished under Contract No. DE-
DE-AC09-76SR00001with the U.S. Department of Energy.

DISCLAIMER

OU'r

TECHNICAL DIVISION
SAVANNAH RIVER LABORATORY

DPST-77-504 657725
ACC. NO. 109826

CC: F. E. Kruesi, Wilm.
R. E. Naylor -
R. F. Ring
J. F. Proctor
C. P. Ross
J. R. Hilley, SRP
D. A. Ward
H. E. Wingo
J. P. Morin
J. H. Hinton
C. H. Ice, SRL
J. M. Boswell
G. F. Merz
R. T. Huntoon
J. A. Smith
S. D. Harris
TIS File

November 15, 1977

M E M O R A N D U M

TO: G. F. MERZ

FROM: W. W. F. YAU WWFYau

RESISTANCE OF REACTOR TOP SHIELD TO TANK VACUUM

INTRODUCTION

Reactor Technology requested[1] an analysis of the effect of a vacuum in the moderator space on the top shield and shield support structure. A vacuum condition could conceivably occur following sudden condensation of a large quantity of steam, or from rapid loss of moderator from a D_2O leak. Earlier analyses of buckling resistances of the reactor tank walls[2,3] concluded that the reactor tank wall could withstand full vacuum. Owing to uncertainties of the top shield resistance, vacuum breakers[4] were installed for relieving negative pressures. For other reasons, replacement of vacuum breakers with rupture disks has been proposed, prompting re-examination of the need for the vacuum breakers.

This work analyzes the structural resistances of the top shield and its support under accident loading conditions. The loading is approximated as a step function, or instant change from one load level to another. Dynamic loading as well as static load changes are considered. The actual load change is estimated to occur in less than 0.5 second; the step function approximation exaggerates the dynamic effect, resulting in a conservative calculation. The numerical results of the study provide a quantitative assessment of structural safety and the necessity of vacuum relief.

SUMMARY

The top shield structures of the three operating reactors have been analyzed for response to loading resulting from a sudden vacuum in the moderator space under the top shield. The results are summarized as follows:

1. The top shield structures including their supporting beams are adequate to sustain the effects of a full vacuum. Under the combined loading of 600 Mark-15 assemblies and imposition of a full vacuum, all structural members respond within elastic limits, hence, the provision of vacuum breakers is not considered essential.

2. The most severely stressed members of the structures are the supporting beams of the top shields in P- and K-Area. Stresses extend to 87% of the yield strength of steel. The supporting beams in C-Area are of different design and are stressed to about 65% yield.

3. Regarding the top shields alone, all designs are equally strong, structurally. For the accident loading, the factor of safety against inelastic deformation is greater than 2.3.

DISCUSSION

The Structure of Top Shields

The top shields for the production reactors at SRP are stainless steel structures of complex tube-sheet assemblies. They are designed in the shape of a circular box stiffened by open ended tubes serving as conduits to the reactor interior. Each of the three top shield designs differs in detail, but the variations are small so their effects on the overall structural behavior are considered secondary. The top shield of the P-reactor is a typical design (Fig. 1): Its primary box-like structure consists of two circular plates. The circular plates are perforated and welded to 841 tubes that occupy the central region of the shield. 673 large tubes are distributed in a uniform triangular pattern, in which 168 small tubes are interspersed in a hexagonal array. Fig. 2 shows typical tube spacings. In the outer region of the shield, structural rigidity is provided by the wrapper plate and 18 web plates.

Accessories of the primary structure are designed mainly for purposes of radiation shielding or easy assembly. Attached to the bottom plate of the top shield are a baffle plate, a deflector plate, four chime plates and a dozen bearing pads. Four lifting lugs and six centering grooves are welded to the top plate. The interior space of the box-like structure is filled with small raschig rings cut from thin-walled tubes of stainless steel. During operation, water circulates throughout the interior by 36 inlet and outlet pipes. These pipes do not stiffen the primary structure, because they are welded only to the top plate of the structure; their lower ends are connected to the baffle plate which is not rigidly fixed to the primary structure.

All tubular conduits of the top shield are in alignment and contact with those in the plenum, so the weight of the plenum, together with that of the hanging fuel assemblies, is transmitted through the contact area to the top shield.

Loading and Support Conditions

Most of the loading on the top shield is transmitted through the bearing ring of the main tank to a set of 12 WF (Wide Flange) cantilevers that are anchored in concrete at -5' elevation. The bearing ring is welded to the flexible expansion ring of the tank wall. Because the expansion ring is highly flexible, it isolates the loading on the top shield from that on the rest of the reactor enclosures. A small portion of the top shield loading is carried by six inlet nozzle pipes that are connected to the plenum. Because the plenum is a much more flexible structure than the top shield, deformation pattern of the former conforms, for small deflection, to that of the latter. For conservative estimation of structural integrity of the top shield and its support structure, the constraining effect of these inlet pipes is not considered in this analysis.

During normal reactor operation, the top shield and the fuel assemblies are submerged in process water, therefore, in the event of a loss-of-coolant accident, there will be a loading increase due to reduction of bouyancy. If the disruption in the supply of coolant is followed by generation and condensation of steam, the top shield and its supporting cantilevers will experience a second surge of loading due to sudden depressurization during steam condensation. The magnitude and duration of the impulsive surge can be conservatively estimated without detailed thermodynamic considerations. The magnitude of the loading increase is limited to one atmosphere, i.e., the maximum reduction of pressure that can occur below the top shield. Since the gas plenum (the space between the top shield and the plenum) maintains a pressure at 5 psi, depressurization below the top shield will cause a downward flow of the coolant that is still held in the annular gaps between the top shield conduits and the housing sleeves of the fuel assemblies. The duration of the pressure impulse is limited to about one-sixth of a second, the time required to flush the coolant through the annular gaps. Estimation of the time duration is shown in Appendix A. Once the annular gaps become free of residual coolant, plenum gas starts to permeate into the tank interior and relieve the pressure on the top shield. The rate of pressure relief is considered much smaller than its buildup in view of the small passages and low upstream pressure for blanket gas flow.

The time history of the loading on the top shield is plotted in Fig. 3. The loading is expressed in terms of uniform pressure over the gross area of the top shield, and the zero time is set at the onset of vapor condensation. To simplify analysis, a single step function (the solid curve in Fig. 3) is used to approximate the pressure variation (the dashed curve) as described in this section. Since the step loading exaggerates the condensation effect (both in magnitude and rate of change) and its attenuation, the analysis will lead to a conservative estimation of stresses imposed. Calculation of the pressure variations is based on the weight and geometry of the top shield and its accessories. Appendix B shows the detail.

The temperature of the top shield structure is not uniform throughout. Inside the top shield, light water circulation is not interrupted, so the temperature is more or less constant around 40°C, and slightly higher near the bottom. The deflector and chime plates below the top shield serve to shield the bottom plate from the high temperature steam prior to condensation. The average metal temperature of the bottom plate is conservatively set at 70°C near the center and 65°C around the edge, hence the wrapper plate is subjected to a temperature gradient of 25°C across its height. Thermal effects due to such a temperature change will be included in this study. In view of the difference in the heat capacities between steel and steam, and the temperature range in consideration, the thermal loading is considered slow in its build-up, so it is a static effect.

Method of Analysis

The structural analysis of the top shield and its supports consists of analyses of effects due to static, dynamic and thermal loading conditions. According to the small deflection theory for perforated plates[5], the elastic responses are linearly independent, thus amenable to separate analyses and superposition. In this study, the static and dynamic loading conditions are obtained by decomposing the loading history as shown in Fig. 3 into a steady-state pressure $p_s = 13.90$ psi, and a sudden pressure $p_d = 16.58$ psi. Thermal effects are included in the static analysis in view of the slow metal response to the temperature changes in air.

The general procedure for analysis of perforated plates[6] is outlined as follows:

STEP 1. Establish an equivalent solid plate having the same dimensions as the perforated plate and effective elastic modulus E^* and Poisson's ratio ν^*. These effective material constants are obtained by modifying the true values of elastic modulus E and Poisson's ratio ν respectively. Precise variation of E^* and ν^* with respect to the geometry of perforation pattern was shown extensively in Reference 7.

STEP 2. Calculate the stresses and deflections according to classical theory of plates. When the perforated plate is part of a structure, as in the case of the top shield, the classical structural analysis applies.

STEP 3. Calculate local stress variation at a particular perforation boundary according to exact theory of elasticity. The perforation is treated as a set of holes in an infinite plate and the stresses obtained in STEP 2 are considered as loading conditions at infinity. Reference 7 also furnished such information in terms of stress concentration factor, i.e., the ratio of the stress at perforation boundary to the nominal stress.

For a plate with a doubly-periodic pattern of circular holes, the perforation geometry can be described by two perforation parameters λ_1^* and λ_2^* defined by d/b_1 and d/b_2 respectively, where d is the hole diameter, b_1 the smallest distance between two holes, and b_2 is the hole spacing measured in a direction perpendicular to b_1. As shown in Fig. 2, the perforation parameters for the top shield plates are

$$\lambda_1^* = 0.63, \; \lambda_2^* = 0.36$$

for $d = 4.385$ inches, $b_1 = 7$ inches and $b_2 = 12.12$ inches. The inside diameter of the large tubes is used for the hole size to account for the stiffening effects of tubes.[8] The variation of the effective material constants in terms of $\lambda_1{}^*$ and $\lambda_2{}^*$ is shown in Fig. 4a,b as reproduced from Reference 7. It indicates

$$E^* = 0.5\ E,\ \nu^* = 0.3\ \nu$$

The effect of the hexagonal pattern of small tubes is not included in consideration of the equivalent plate. Because of the small perforation parameters ($\lambda_1{}^* = 0.13$, $\lambda_2{}^* = 0.07$), the change in material constants is insignificant.

When the top shield structure is treated as a closed box made of two equivalent solid plates stiffened by a wrapper plate and a set of internal bracings, its flexural rigidity is

$$D^* = \frac{E^* H^2 h}{2(1-\nu^{*2})} \left(1 - 2\frac{h}{H} + \frac{4}{3}\frac{h^2}{H^2}\right)$$

where h = 1 inch and H = 40 inches are the thickness of the plates and the height of the top shield respectively. Derivation of D* is shown in Appendix C.

Static Analysis

The simply supported structure of the shield is decomposed into two equivalent solid plates and a wrapper plate for separate analysis. At their boundaries, the radial forces Q_{aB} and Q_{aT}, and bending moments M_{aB} and M_{aT} per unit length of the circumference are unknown reactions to be determined by consideration of consistent deformation. The subscripts B and T signify quantities pertaining to the bottom and top plates respectively, and the subscript a indicates the radius (or circumference) of the plates. External loading applied to one of the plates is transmitted by the connecting tubes to the other. It can be shown that these tubes can effectively transmit about one half of the load; hence,

$$\begin{aligned} M_{aB} &= M_{aT} = \frac{1}{2} M_a \\ Q_{aB} &= Q_{aT} = Q_a \\ p_{sB} &= p_{sT} = \frac{1}{2} p_s \end{aligned} \tag{1}$$

In cylindrical coordinates (r,z) with the center of the top shield structure as their origin, the elastic responses of the plates, based on the small deflection theory of plates[9], can be readily obtained as

$$w = \frac{a^2-r^2}{64D^*} \left[p_s a^2 \left(\frac{5+\nu^*}{1-\nu^*} - \frac{r^2}{a^2}\right) + \frac{32}{1+\nu^*} M_a\right]$$

$$u = \pm \left[\frac{H}{2}\frac{dw}{dr} + \frac{(1-\nu^*)Q_a}{E^*h} r\right] \tag{2}$$

$$\sigma_r = \mp \frac{1}{Hh} \left[\frac{3+\nu^*}{16} p_s a^2 \left(1-\frac{r^2}{a^2}\right) + M_a - Q_a H\right]$$

$$\sigma_\Theta = \mp \frac{1}{Hh} \left[\frac{1+3\nu^*}{16} p_s a^2 \left(\frac{3+\nu^*}{1+3\nu^*} - \frac{r^2}{a^2}\right) + M_a - Q_a H\right]$$

where u and w are the displacement components in the directions of r and z, σ_r and σ_Θ are the radial and circumferential stresses, and the upper and lower signs refer to the top and bottom plates respectively.

The elastic responses of the wrapper plate under edge loading Q_a and M_a are characterized solely by its radial displacement $\tilde{u}$. Its governing differential equation (10) has the following solution satisfying the boundary conditions:

$$\tilde{u} = b_1 \sin\frac{2\lambda Z}{H} \cosh\frac{2\lambda Z}{H} + b_2 \cos\frac{2\lambda Z}{H} \sinh\frac{2\lambda Z}{H}$$

$$\lambda^4 = \frac{3(1-\nu^2)H^4}{16a^2\tilde{h}^2} \tag{3}$$

$$b_1 = \frac{3(1-\nu^2)H^2}{2E\lambda^3\tilde{h}^3}\left[\frac{Q_a H \sin\lambda\cosh\lambda - M_a\lambda(\cos\lambda\cosh\lambda + \sin\lambda\sinh\lambda)}{\sinh 2\lambda - \sin 2\lambda}\right]$$

$$b_2 = \frac{3(1-\nu^2)H^2}{2E\lambda^3\tilde{h}^3}\left[\frac{Q_a H \cos\lambda\sinh\lambda - M_a\lambda(\cos\lambda\cosh\lambda - \sin\lambda\sinh\lambda)}{\sinh 2\lambda - \sin 2\lambda}\right]$$

where $\tilde{h}$ is the thickness of the wrapper plate.

For consistent deformation of the plates along their common boundaries, i.e., $r = a$ and $Z = \pm 0.5H$, the geometrical conditions (Fig. 5) require

$$u + \tilde{u} = \frac{1}{2}(T_B - T_T)\alpha a \qquad (4)$$

$$\frac{d\tilde{u}}{dZ} = \frac{dw}{dr}$$

where the right hand side of the first equation is the radial change due to the difference of temperatures T_B and T_T for the bottom and top plates respectively, and α is the coefficient of thermal expansion for stainless steel.

Substitution of the elastic results of Eq. (2) and (3) in Eq. (4) leads to a set of equations for the solutions of unknown reactions M_a and Q_a.

$$Q_a H(\frac{f_1}{\lambda} + \delta) - M_a(f_2+\delta) = \frac{8\lambda^2 \alpha a D}{H^2}(T_B - T_T) + \frac{\delta}{8} p_s a^2$$

$$Q_a H f_2 - M_a(2\lambda f_3 + \delta) = \frac{\delta}{8} p_s a^2 \qquad (5)$$

$$\delta = \frac{8\lambda^2 aD}{(1+\nu^*)HD^*}, \quad D = \frac{E\tilde{h}^3}{12(1-\nu^2)},$$

$$f_1 = \frac{\cosg 2\lambda - \cos 2\lambda}{\sinh 2\lambda - \sin 2\lambda}, \quad f_2 = \frac{\sinh 2\lambda + \sin 2\lambda}{\sinh 2\lambda - \sin 2\lambda}, \quad f_3 = \frac{\cosh 2\lambda + \cos 2\lambda}{\sinh 2\lambda - \sin 2\lambda}$$

For the top shield structure in consideration the value of λ is sufficiently large, such that f_1, f_2 and f_3 are all close to unity, and δ is negligibly small, so the solution to Eq. (5) can be approximated by

$$M_a = \frac{8\lambda^2 \alpha a D}{H^2}(T_B - T_T) + \frac{(\lambda-1)\lambda a D}{(1+\nu^*)HD^*} p_s a^2$$

$$Q_a = \frac{16\lambda^3 \alpha a D}{H^3}(T_B - T_T) + \frac{(2\lambda-1)\lambda^2 a D}{(1+\nu^*)H^2 D^*} p_s a^2 \qquad (6)$$

The maximum stresses in the wrapper plate occur at the edges joining the flat plates. The maximum bending and shearing stresses are respectively,

$$\tilde{\sigma}_{max} = \frac{3M_a}{\tilde{h}^2}, \quad \tilde{\tau}_{max} = \frac{3Q_a}{2\tilde{h}} \tag{7}$$

For the equivalent circular plates, the maximum stresses are tensile for the bottom plate and compressive for the top plate. At the center of each plate, $\sigma_r = \sigma_\Theta = S_{max}$, and

$$S_{max} = \frac{1}{Hh}\left[\frac{3+\nu^*}{16} - \frac{(2\lambda^2-2\lambda+1)\lambda aD}{(1+\nu^*)HD^*}\right]p_s a^2 - \frac{8(2\lambda-1)\lambda^2\alpha aD}{H^3h}(T_B-T_T) \tag{8}$$

Stress concentration at the rim of a hole near the center is considered in Reference 7. The variation of stress with respect to the perforation parameter is reproduced in Figure 4c, where for $\lambda_1^* = 0.63$, the stress concentration factor is less than 3, or

$$\sigma_{max} \leq 3S_{max} \tag{9}$$

The structural data of the top shield are listed as follows.

$E = 30(10)^6$ psi $\qquad E^* = 15(10)^6$ psi

$\nu = 0.3$ psi $\qquad \nu^* = 0.09$

$\alpha = 17(10)^{-6}$ in./in-^oC

$h = 1$ in.

$H = 40$ in.

$\tilde{h} = 0.5$ in.

$a = 112$ in.

$\lambda = 3.435$

$D = 0.3434(10)^6$ lb-in.

$D^* = 12098(10)^6$ lb-in.

Using these data and the loading conditions of p_s = 13.9 psi and $T_B - T_T = 25^{o}C$, the static responses are calculated as

$$M_a = 1071 \text{ in-lb/in.}$$

$$Q_a = 187.6 \text{ lb/in.}$$

$$\tilde{\sigma}_{max} = 12.35 \text{ ksi}, \quad \tilde{\tau}_{max} = 0.56 \text{ ksi}$$

$$S_{max} = 0.68 \text{ ksi}, \quad \sigma_{max} = 2.04 \text{ ksi}$$

The maximum stress $\tilde{\sigma}_{max}$ is due to bending of the wrapper plate along the circumferential edges. Eq. (6) shows that the thermal effect of a $25^{o}C$ temperature change contributes about 90% of the edge bending, therefore $\tilde{\sigma}_{max}$ is mostly a thermal stress. It is noted that the effect of edge bending on the overall lateral deflection of the top shield, as indicated by the first equation of Eq. (2), is less than 4%.

Dynamic Analysis

The transverse motion of the top shield to a suddenly applied pressure p_d is governed by (11)

$$\frac{D^*}{a^4}\frac{1}{x}\frac{\partial}{\partial x}\left\{x\frac{\partial}{\partial x}\left[\frac{1}{x}\frac{\partial}{\partial x}\left(x\frac{\partial w}{\partial x}\right)\right]\right\} + \rho\frac{\partial^2 w}{dt^2} = p_d, \quad t \geqslant 0 \tag{10}$$

where x = r/a is the dimensionless radial coordinate, t is the time variable, and ρ is the mass per unit area of the structure. The solution to Eq. (10) for the simply supported structure that is initially stationary is

$$W(x,t) = \frac{P_d a^4}{D^*}\sum_{n=1}^{\infty} C_n f_n(x)(1-\cos\omega_n t) \tag{11}$$

with

$$f_n(x) = I_o(k_n)\, J_o(k_n x) - J_o(k_n) I_o(k_n x)$$

$$C_n = \frac{1}{k_n^4}\frac{\int_o^1 x f_n dx}{\int_o^1 x f_n^2 dx}, \qquad \omega_n = \frac{k_n^2}{a^2}\sqrt{\frac{D^*}{\rho}}$$

where k_n are the characteristic values of

$$\frac{J_1(k_n)}{J_o(k_n)} + \frac{J_1(k_n)}{J_o(k_n)} = \frac{2k_n}{1-\nu^*} \tag{12}$$

and J_m and I_m for m = 0 or 1 are Bessel and modified Bessel functions of m-th order. The dynamic response written in the form of Eq. (11) represents the whole spectrum of vibrating modes with deflection shapes $f_n(x)$ and circular frequencies $\omega_n/(2\pi)$. The effect of each modal component on the overall motion is determined by the participation factor C_n. The value of C_n diminishes with increasing n, and for a prescribed accuracy, the number of modes required for approximation increases with structural flexibility.

The solution to the characteristic Eq. (12) is graphically represented by the intersections of the straight line with the curves (Fig. 6). For the top shield, the first three roots are

$$k_1 = 2.4, \quad k_2 = 5.43, \quad k_3 = 8.58$$

The corresponding circular frequencies and participation factors are

$$\frac{\omega_1}{2\pi} = 31.6 \text{ cps}, \quad \frac{\omega_2}{2\pi} = 204 \text{ cps}, \quad \frac{\omega_3}{2\pi} = 509 \text{ cps},$$

$$C_1 = 31.51(10)^{-3}, \quad C_2 = 0.10(10)^{-3}, \quad C_3 = 6.3(10)^{-6}$$

These participation factors indicate that use of the fundamental mode for the overall response introduces an error less than 1%, so Eq. (11) is simplified by

$$W(x,t) = C_1 p_d \frac{a^4}{D^*} f_1(x)(1-\cos\omega_1 t)$$

whose maximum deflection shape is

$$W_{max}(x) = 2C_1 p_d \frac{a^4}{D^*} f_1(x)$$

By definition (Appendix C), the stress components are

$$\sigma_r(x) = 2C_1 p_d \frac{a^2}{Hh} \left[f_1''(x) + \frac{\nu^*}{x} f_1'(x) \right]$$

$$\sigma_\theta(x) = 2C_1 p_d \frac{a^2}{Hh} \left[\nu^* f_1''(x) + \frac{1}{x} f_1'(x) \right]$$

where the primes denote the derivatives.

The maximum stress occurs at the center of the circular plates, and both stress components are of equal magnitude. Computed from the following data

$$p_d = 16.58 \text{ psi}, \quad \nu^* = 0.09, \quad f_1'(0) = -6.094$$

$$a = 112 \text{ inches}, \quad H = 40 \text{ inches}, \quad h = 1 \text{ inch}$$

the maximum effective stress is

$$S_{max} = \sigma_r(0) = \sigma_\theta(0) = 2.18 \text{ ksi}$$

and the highest stress due to concentration at the hole rim is

$$\sigma_{max} = 3 \, S_{max} = 6.54 \text{ ksi}$$

Analysis of Supporting Beams

The top shield is supported on 12 wide flange beams equally spaced along its circumference and in radial directions. These beams were anchored in 12 cave-like recesses in the thick concrete wall surrounding the reactor tank. Each beam protrudes about one foot outside the cylindrical wall and acts like a cantilever under loading (Fig. 7). The reaction R for each beam due to static and dynamic loading on the top shield at any time is

$$R = \frac{1}{12} \left[(p_s + p_d) \, A + \int_A p \, \frac{\partial^2 w}{\partial t^2} \, dA \right]$$

where A is the area of the top shield, and the integral represents the inertial effect of the structure. It can be shown that the time dependent integral has a maximum value of cp_dA, so the maximum load on the beam is

$$R_{max} = \frac{\pi a^2}{12}\left[p_s + (1+C)\ p_d\right]$$

where
$$C = 4C_1K_1^{\ 4}\ J_o(K_1)\left[\frac{J_o(K_1)}{1-\nu^*} - \frac{J_1(K_1)}{K_1}\right]$$

For p_s = 13.90 psi, p_d = 16.58 psi, a = 112 inches, Eq. (15) gives C = 0.73 and

$$R_{max} = 140{,}000 \text{ lbs.}$$

The beams are of 14 WF 142 cross-section according to the P-reactor design, and each beam is anchored by four 2 inch diameter bolts at distances of 22 and 56 inches from the loading end. By equilibrium considerations, the tensile stress in the remote bolts, the bending stress in the flange, and the shearing stress in the web of the wide flange section have, respectively, the following maximum values:

$$\sigma_{bolt} = \frac{22}{56-22}\left(\frac{140}{2\pi}\right) = 14.4 \text{ ksi}$$

$$\sigma_{max} = \frac{140(22)}{226.7} = 13.8 \text{ ksi}$$

$$\tau_{max} = \frac{140}{1672.2(8)}\left[\frac{15.5}{0.68}\ (14.75^2-12.62^2) + 12.62^2\right] = 15.6 \text{ ksi}$$

Structural Resistance

The material used for the construction of all top shields is 304 stainless steel. For the supporting beams, ASTM A36 carbon steel is the primary structural material. Other steels are used for pins, nuts, padding plates, etc. Static strengths of the structural materials tested at room temperature are listed as follows.

Steel	Strength in ksi	
	Yield	Tensile
SS 304	30	75
A 36	36	58

Steel resistance is generally higher under dynamic loading but lower at higher temperatures. For the range of temperatures considered in this study, variation of material strength is not appreciable.

Combining the numerical results of the static and dynamic analyses of the top shield structure, the maximum stresses are less than 13 ksi in the wrapper plate and 8.6 ksi in the perforated plates. So the top shield structure of the P-reactor is elastically resistant to a loading about 2.3 times that considered in the study. Resistance of the top shield for the C-reactor is considered at least as great. Structurally, the only design difference involves the location of support. The C-design uses 12 bearing brackets welded to the upper side of the wrapper plate. Since the wrapper plate is thicker in regions where the bearing brackets and the web plates are attached, application of the results of the P-design is hence conservative.

Stress results of the supporting beams of the P-reactor design indicate that the web sections of the wide flange beams will be most severely stressed to 87% of the elastic limit of steel under dynamic loading. The level of stress would be considered too high for design loading, but allowable under accident conditions. For the C-reactor design, the supporting beams (14 WF 342) and the anchoring bolts (2.25 inch diameter) are considerably heavier. The spacing of the anchoring bolts is also different; as a result the most limiting stress (23.3 ksi) is in the remote anchoring bolts and well within the yield strength.

WWFY:vpb

REFERENCES

1. Hinton, J. H., "Reactor Tank Vacuum Relief Without Vacuum Breakers," RTA 1374R, March, 1977.

2. Walker, J. W., "Collapsing Pressure of RPLK Reactor Tanks, "DPST-62-178, March, 1962

3. Ward, D. A., "Collapse Pressure of RPLK Tanks," DPST-62-394, December, 1962.

4. Black, J. E., "Vacuum Breaker Replacement" RTW-221, January, 1975.

5. Koiter, W. T., "Stress Distribution in an Infinite Elastic Sheet with a Doubly-Periodic Set of Equal Holes," in "Boundary Problems in Differential Equations," pp. 191-213, Univ. Wisconsin Press, Madison, 1960.

6. O'Donnell, W. J. and Langer, B. F., "Design of Perforated Plates, pp. 307-320, J. of Engineering for Industry, August, 1962.

7. Meijers, P., "Doubly-Periodic Stress Distributions in Perforated Plates," Thesis, Delft, 1967.

8. O'Donnell, W. J., "The Effect of the Tubes on Stresses and Deflections In U-Tube Steam Generator Tube Sheets," pp. 89-97, Bettis Technical Review, WAPD-BT-21, November, 1960.

9. Timoshenko, S., and Weinowsky-Krieger, S., "Theory of Plates and Shells," Chapter 3, McGraw-Hill, New York, 1959.

10. Chapter 15 of Reference (9).

11. Prescott, J., "Applied Elasticity," p. 581, Dover, New York, 1961.

12. Pai, S. J., "Viscous Flow Theory," p. 43, Vol. II, D. Van Nostrand, New York, 1957.

13. Knoebel, D. H., Yau, W. W. F., and Muhlbaier, D. R., "Reactor Vent Limitations for ECW Flow," DPST-74-240, February, 1974.

14. Macafee, I. M., and Nomm, E., "Mark 15 Design Studies," DPST-72-509, October 1972.

15. Chapter 2 of Reference (9).

APPENDIX A

FLOW OF RESIDUAL COOLANT IN ANNULAR GAPS

In a loss-of-coolant accident, the flow of water in the annular gaps between the housing sleeves of the fuel assemblies and the conduits in the top shield is impeded by shear resistance. For the possible range of flow velocity in the gaps caused by a leak of 75,000 gpm, the flow is turbulent, and the viscous resistance (12) is estimated by

$$R_f = kv^2, \quad k = 0.04\rho A \left(\frac{\mu}{\rho h_f v}\right)^{\frac{1}{4}} \tag{A1}$$

where ρ is the mass density of water, A is the liquid-metal contact area, μ is the coefficient of water viscosity, h is the gap width in the 4" positions and ν is the mean flow velocity. Water on top of the top shield does not flow down the sleeve annulus because the sleeves extend above the shield 6 inches, equal to the weir height. This water will flow around the outside edge of the shield to the tank, but will require 2 seconds to vent. The annular flow analyzed here vents first, and is controlling.

Let F be the driving force due to steam condensation and the gas plenum pressure, and W be the weight of water in gaps; then the downward flow by first order approximation is simply

$$F + W - R_f = \frac{W}{g}\frac{dv}{dt} \tag{A2}$$

where g is the gravitational acceleration. If k is considered constant at some average value of v, the solution to the equation of motion becomes

$$v = \frac{\alpha W}{kg}\tanh(\alpha t), \quad \alpha = \frac{g}{W}\ k(F+W)^{\frac{1}{2}} \tag{A3}$$

Using ρ = 66 lbm/ft^3, A = 5100 ft^2, h = 0.0055 ft and μ = 0.593(10)$^{-5}$ lbm-sec/ft^2, Eq. (A1) gives k = 15 at v = 10 ft/sec. For F = 11820 lbs, and W = 870 lbs, the flow velocity is

$$v = 29\tanh(16.15t) \tag{A4}$$

where t is in seconds. The maximum mean velocity is 29 ft/sec. The displacement in feet is obtained by integration of Eq. (A4),

$$S = 1.79\ \ell n(\cosh 16.15t) \tag{A5}$$

To flush the water through the top shield, S = 3.33 ft, the time required is t = 0.16 sec.

APPENDIX B

TOP SHIELD LOADING CALCULATION

The unit load on the top shield is based on its gross area (39400 sq. in., Dwg-W131857) and the net downward forces on the structure before and during the event of a large scale leak (D_2O at 75,000 gpm). Prior to the accident, the net load is equal to the weight of the hardware minus bouyancy. The total weight and bouyancy forces are listed as follows:

Plenum with D_2O (13)	+	61100 lbs
Top shield with H_2O	+	206600 "
USH and bottom fitting	+	21000 "
Full charge, Mark 15 (14)	+	333000 "
Total Weight	+	621700 lbs

Bouyancy of top shield	-45600 lbs
Bouyancy of assemblies	-28600 "
Total Bouyancy	-74200 lbs

$$\text{Net Unit load} = \frac{621700 - 74200}{39400} = 13.90 \text{ psi}$$

As the level of moderator recedes (at a rate about one foot per second with no emergency coolant inflow), bouyancy forces diminish rapidly during the early stage. Its effect on the top shield is an increase of pressure to a level not greater than 15.78 psi.

Prior to onset of steam condensation, the pressure due to steam generation tends to reduce top shield loading. The magnitude of steam pressure is assumed to be small because of large leakage.

TOP SHIELD FLEXURAL RIGIDITY

For small deflection, bending of the top shield introduces compressive and tensile stresses in the top and bottom plates. Choosing z as the distance from the neutral plane, i.e., the plane of zero stress if the shield is solid, for symmetrical bending of a circular plate, the radial and circumferential stresses, σ_r and σ_θ, in the plate are functions of the derivatives of the lateral deflection w[15],

$$\sigma_r = \frac{Ez}{1-\nu^2}\left(\frac{d^2w}{dr^2} + \frac{\nu}{r}\frac{dw}{dr}\right)$$

$$\sigma_\theta = \frac{Ez}{1-\nu^2}\left(\nu\frac{d^2w}{dr^2} + \frac{1}{r}\frac{dw}{dr}\right)$$

where E and ν are material constants, and r is the radial coordinate from the plate center. By definition, the radial and circumferential moments are

$$M_r = 2\int_{\frac{1}{2}H-h}^{\frac{1}{2}H} z\sigma_r dz = D\left(\frac{d^2w}{dr^2} + \frac{\nu}{r}\frac{dw}{dr}\right)$$

$$M_\theta = 2\int_{\frac{1}{2}H-h}^{\frac{1}{2}H} z\sigma_\theta dz = D\left(\nu\frac{d^2w}{dr^2} + \frac{1}{r}\frac{dw}{dr}\right)$$

where

$$D = \frac{EH^2h}{2(1-\nu^2)}\left(1-2\frac{h}{H} + \frac{4}{3}\frac{h^2}{H^2}\right)$$

is the flexural regidity, h and H are the plate thickness and the top shield height respectively.

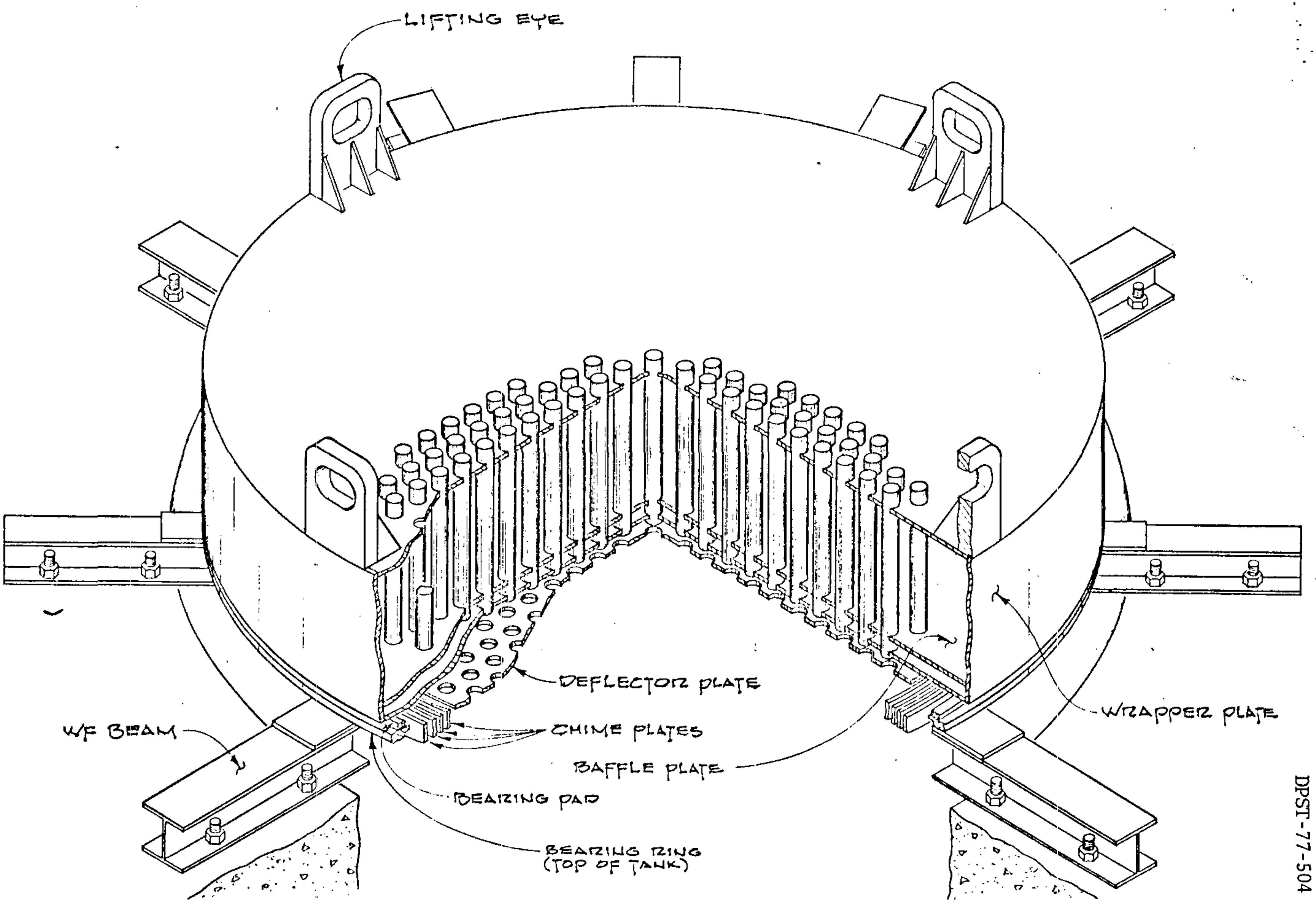

FIGURE 1 - P-REACTOR TOP SHIELD

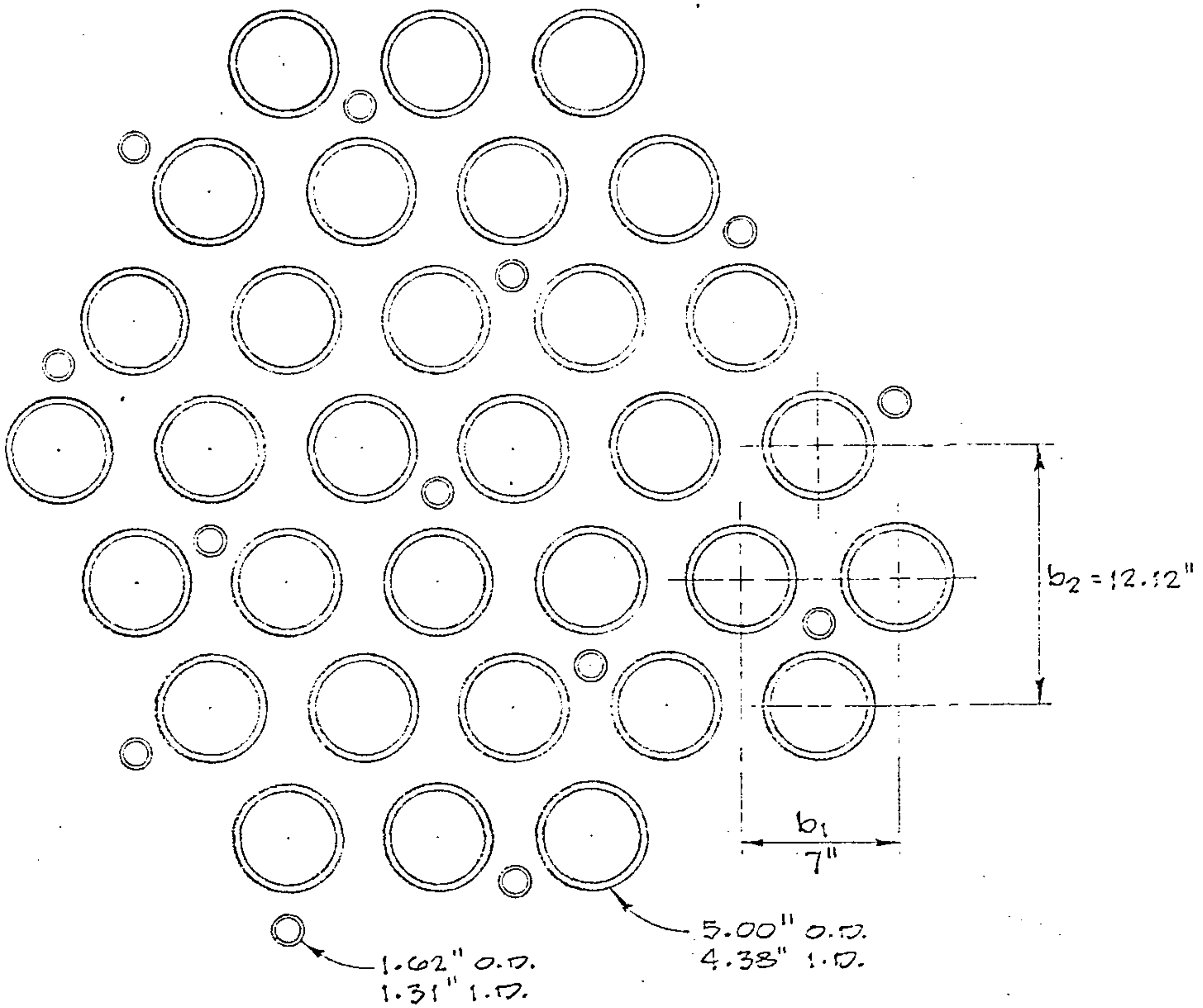

FIGURE 2 - TOP SHIELD TUBE PATTERN

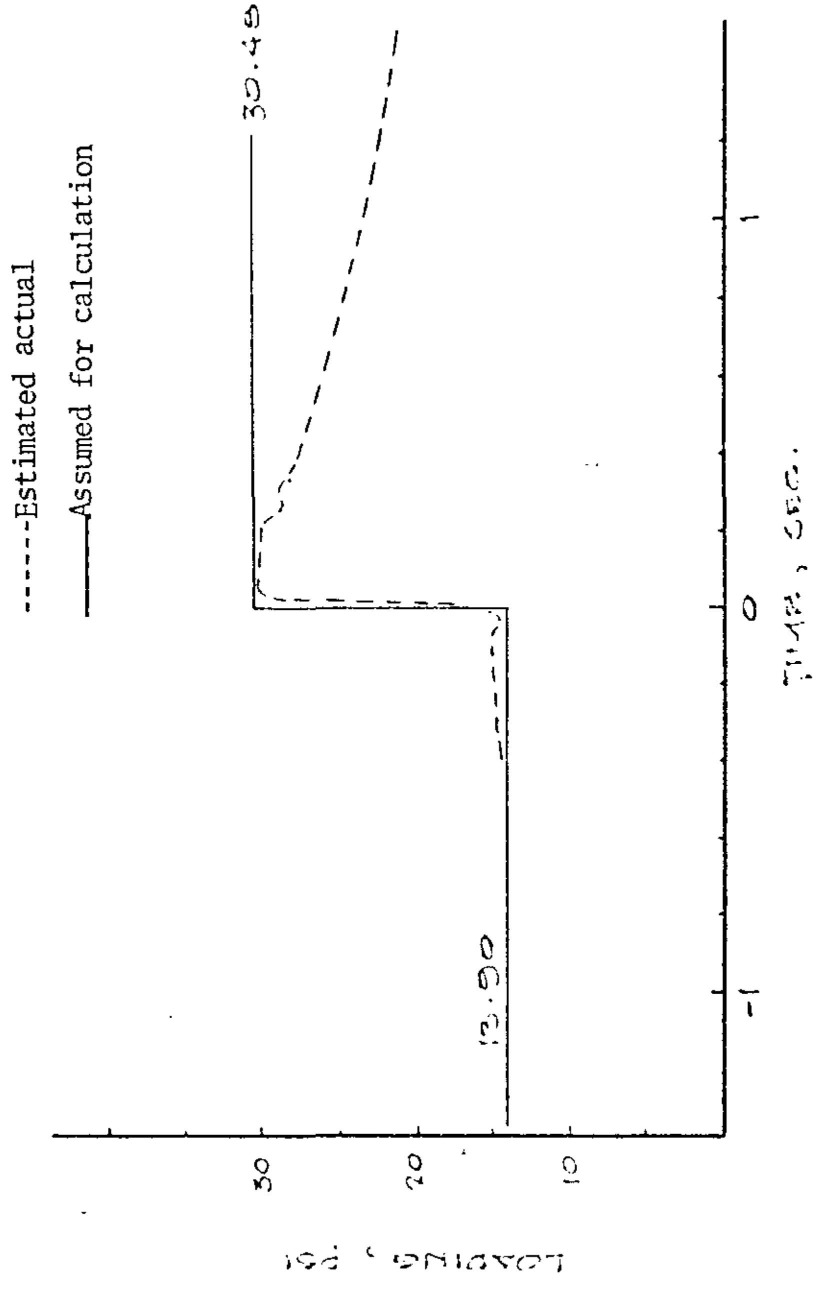

FIGURE 3 - LOADING HISTORY

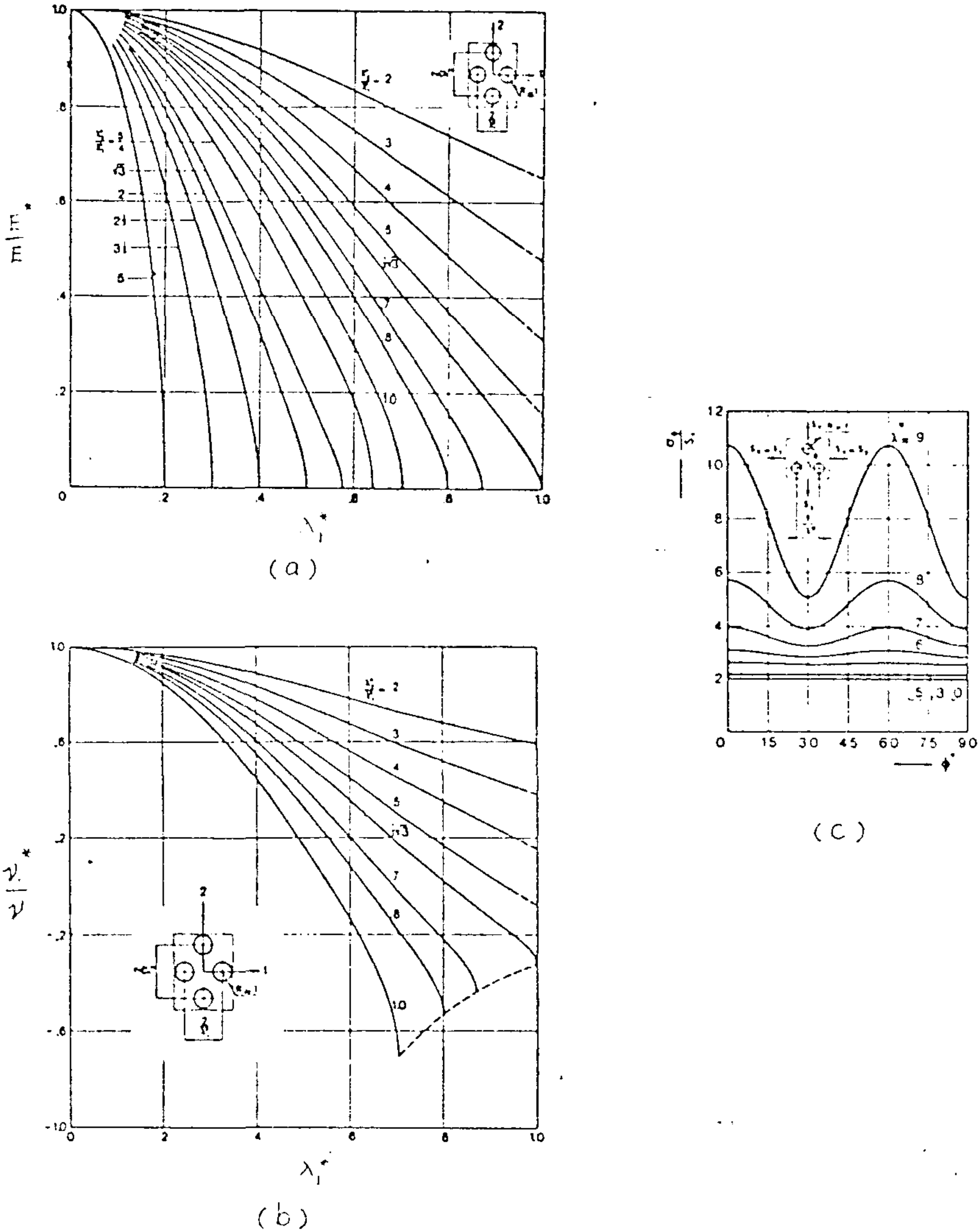

FIG. 4 EFFECTIVE PLATE CONSTANTS

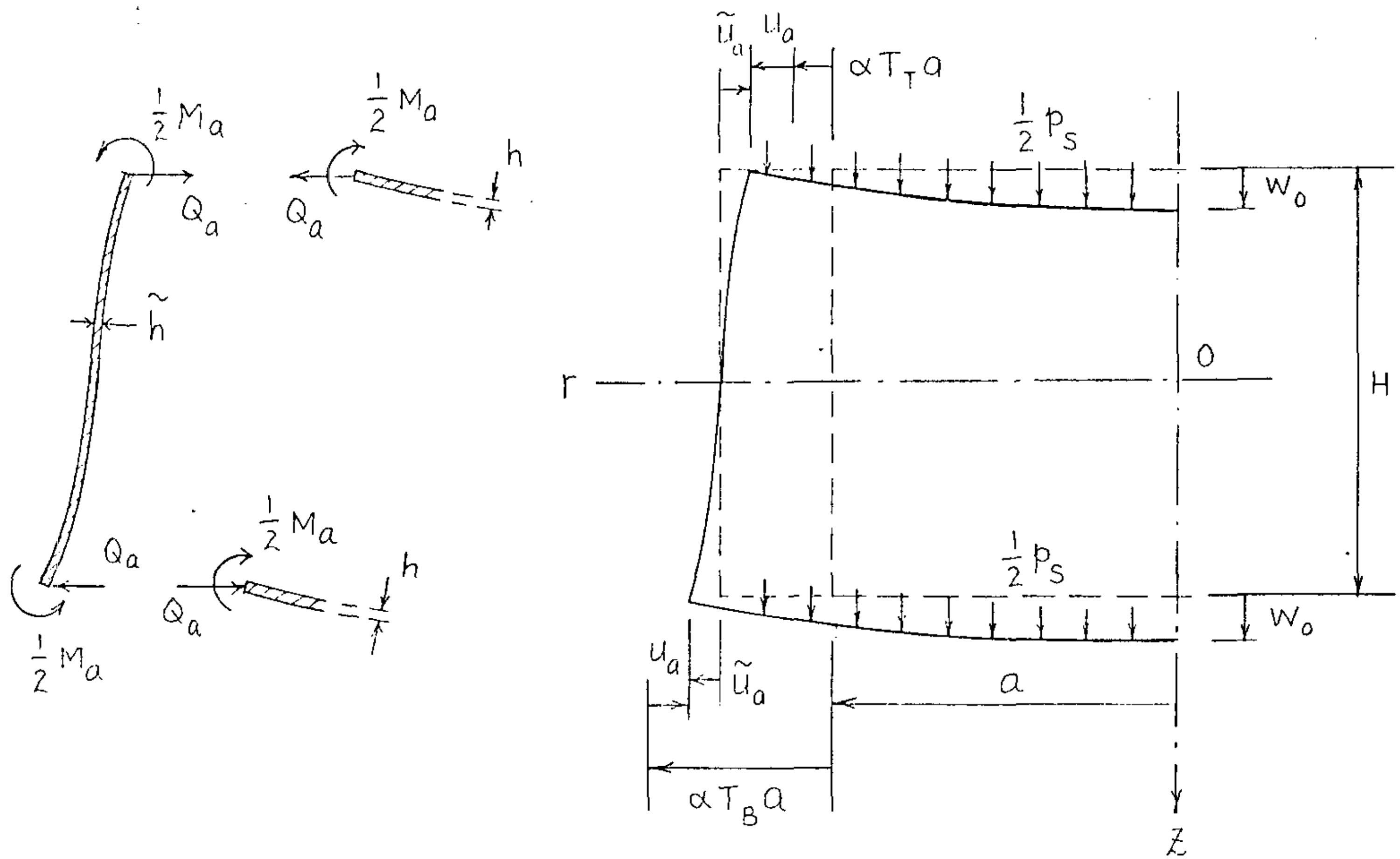

FIG. 5 TOP SHIELD DEFORMATION

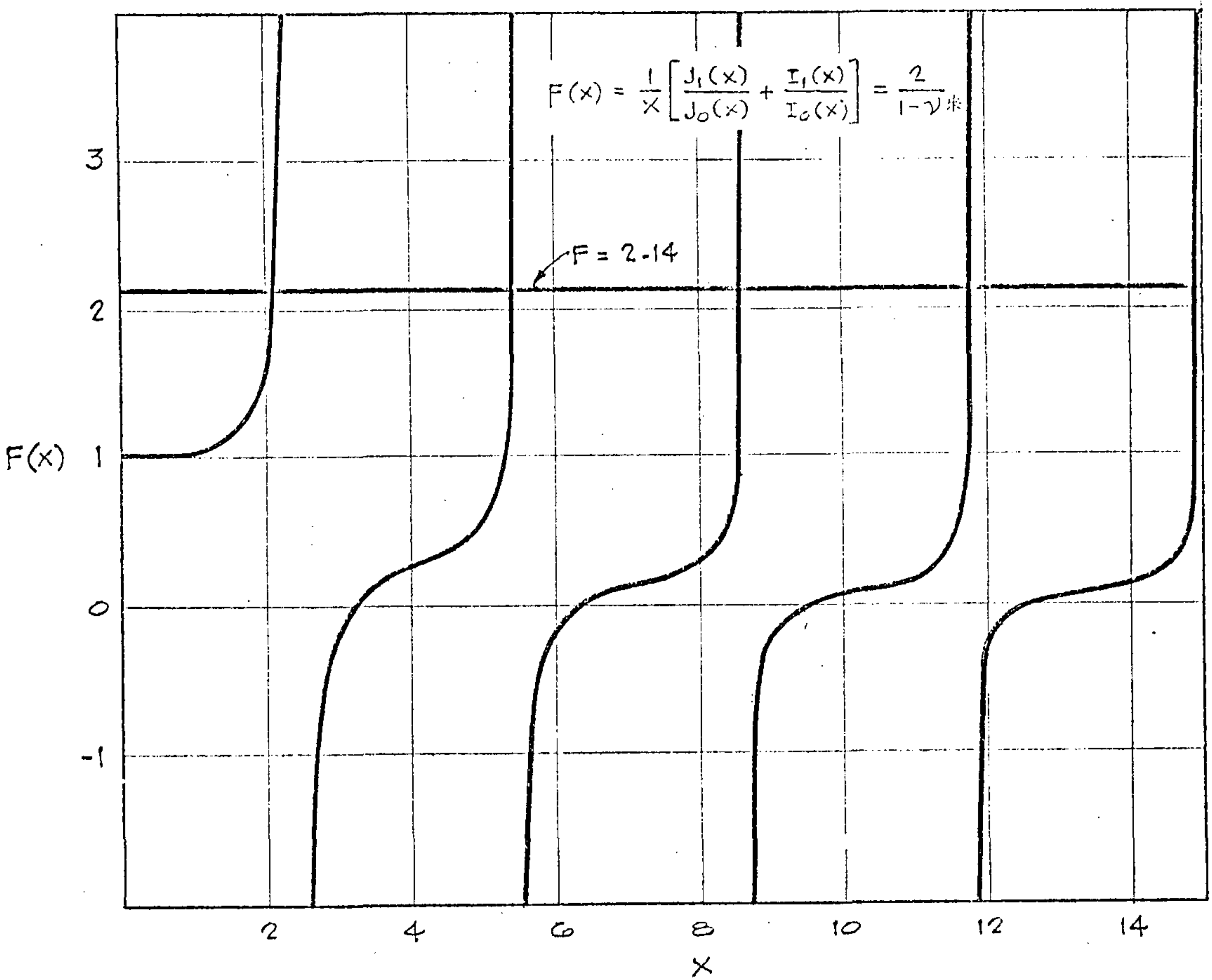

FIGURE 6 - VIBRATIONAL CHARACTERISTICS

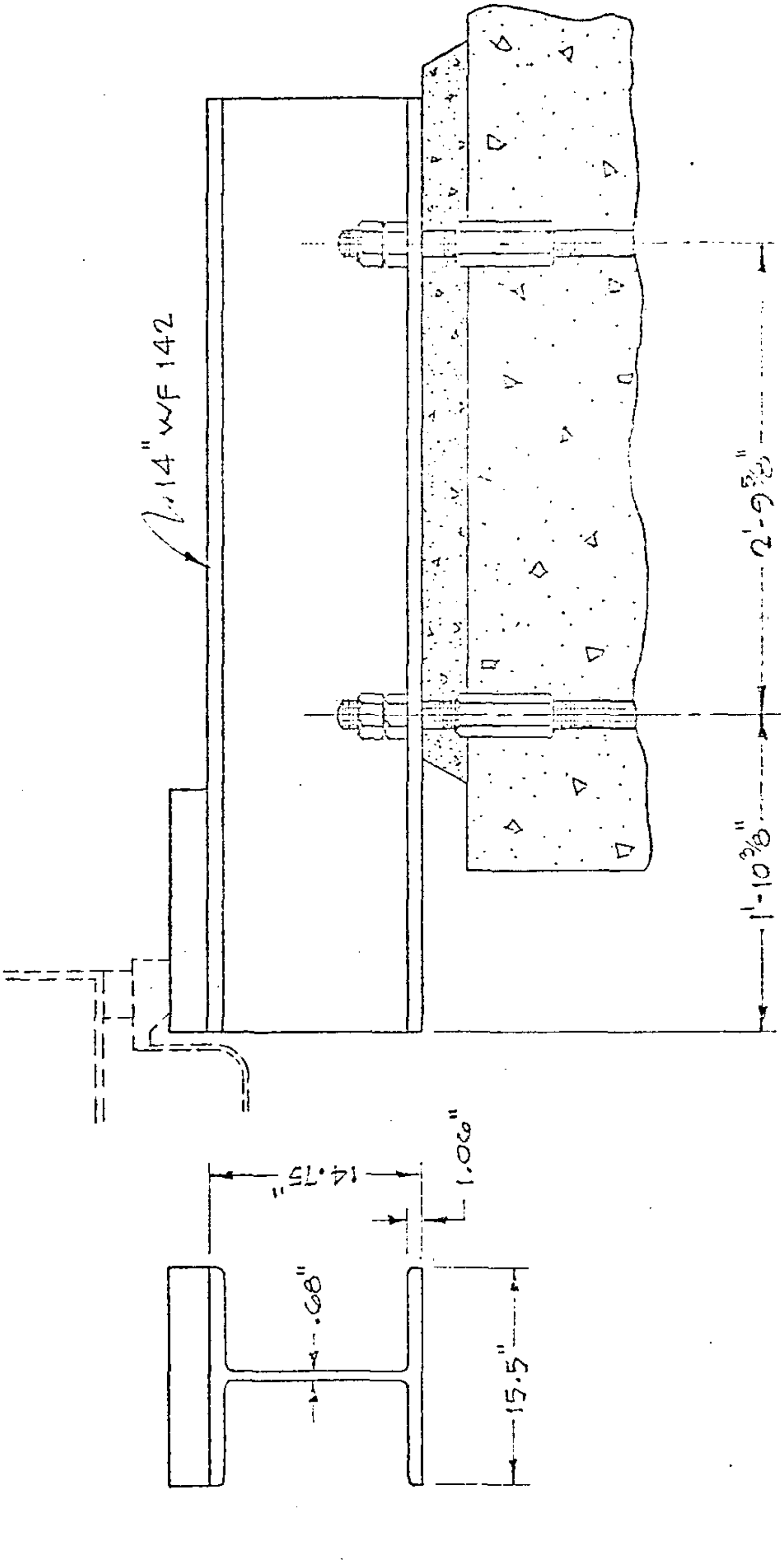

FIGURE 7 - P-REACTOR TOP SHIELD SUPPORT